

# The growth with energy of vector meson photo-production cross-sections and low $x$ evolution

---

**Martin Hentschinski**<sup>\*†</sup>

*Departamento de Actuaría, Física y Matemáticas, Universidad de las Américas Puebla, Santa Catarina Martir, 72820, Cholula, Puebla, Mexico*

*E-mail:* [martin.hentschinski@udlap.mx](mailto:martin.hentschinski@udlap.mx)

We investigate the energy dependence of the exclusive photo-production cross-sections of vector mesons  $J/\Psi$  and  $\Upsilon$  on protons. In particular we are interested in the question whether their energy dependence has a description in terms of perturbative low  $x$  (i.e. BFKL) evolution. As an update to the original publication [1] we include recent LHCb 13 TeV results in our comparison with data.

*XXV International Workshop on Deep-Inelastic Scattering and Related Subjects*

*3-7 April 2017*

*University of Birmingham, UK*

---

<sup>\*</sup>Speaker.

<sup>†</sup>Financial support by the workshop organizers and CONACyT-Mexico grant number CB-2014-241408 is gratefully acknowledged

## 1. Introduction

Exclusive photo-production of vector mesons  $J/\Psi$  and  $\Upsilon$  is one of the few processes which currently allow to investigate the proton at ultra-small values of  $x$ , down to  $x \simeq 5 \cdot 10^{-6}$ . This process was originally measured at the HERA experiments by both H1 and ZEUS collaborations in  $ep$  collisions; at the LHC it is now further possible to extract the corresponding cross-section from photon induced reactions in  $pp$  and in ultra-peripheral  $pPb$  collisions (UPCs). The hard scale of this process is provided by the mass of the heavy quark, charm ( $J/\Psi$ ) and bottom ( $\Upsilon$ ). Exploring the region of ultra-small  $x$  is of interest for a number of reasons: first of all it allows to constrain the shape of the – in this region of phase space little known – gluon distribution function[2]. While fixing the shape of the gluon distribution in this region provides valuable information, the ability to realize such a fit does not immediately imply a proof of the validity of dilute DGLAP evolution in this region of phase space. Indeed DGLAP evolution – which is known to suffer from instabilities in the ultra-small  $x$  region – occurs only between two scales: the  $J/\Psi$  and the  $\Upsilon$ . We therefore argue that in order to identify the dominant physics in this region it is more interesting to study these observables using low  $x$  evolution equations *i.e.* to fix the input gluon at some low  $x$  value in the range  $x \simeq 10^{-2} - 10^{-4}$  (mainly using inclusive HERA data) and to evolve this input with evolution kernels derived from perturbative QCD down to  $x$  values characteristic for vector meson production in UPCs at the LHC. A prominent example of low  $x$  evolution is provided by the non-linear BK/JIMWLK evolution equation. These evolution equations are of particular interest since they allow to evolve the gluon deep into the saturated region, where the non-linear terms slow down the observed growth of the gluon at low  $x$  and ultimately bring it to hold. While the potential of such evolution equations (and corresponding saturation models which mimic such evolution equations) to describe  $J/\Psi$  and  $\Upsilon$  photo-production data has been demonstrated [3], it is nevertheless not clear whether saturation effects manifest themselves already at the currently accessible values of  $x$  or whether one mainly observes a continuation of low  $x$  evolution in the dilute limit. To answer such question it is therefore more valuable to study linear, *i.e.* BFKL, evolution. Inability of linear evolution to describe  $J/\Psi$  and  $\Upsilon$  data *combined* with a successful description by non-linear evolution would provide then a far more solid evidence for the presence of saturation effects. In the following we present some details of a recently performed BFKL studies; for a complete discussion we refer to [1], while we would like to point out that the comparison to experimental results to be shown below contains as an update LHCb data not included in the original publication.

## 2. The NLO BFKL gluon density

The construction of the BFKL unintegrated gluon is closely based on the HERA fit of [4], which uses the following model of the proton impact factor

$$\Phi_p \left( \frac{q^2}{Q_0^2}, \delta \right) = \frac{\mathcal{C}}{\pi \Gamma(\delta)} \left( \frac{q^2}{Q_0^2} \right)^\delta e^{-\frac{q^2}{Q_0^2}}. \quad (2.1)$$

The free parameters of the model ( $Q_0, \delta, \mathcal{C}$ ) are fixed by a fit to the proton structure  $F_2$  in the low  $x$  region,  $x < 10^{-2}$ ; we will use  $Q_0 = 0.28$  GeV,  $\delta = 6.5$  and  $\mathcal{C} = 2.35$  together with a value of  $\Lambda_{\text{QCD}} = 0.21$  GeV as the reference scale of the QCD running coupling; the numbers of flavors will

be fixed to  $n_f = 4$  throughout. Using this input distribution, an unintegrated gluon density can be extracted from the original  $F_2$  fit, given by the following convolution of proton impact factor and BFKL Green's function [5]

$$G(x, \mathbf{k}^2, Q_0^2) = \int \frac{d\mathbf{q}^2}{q^2} \mathcal{F}^{\text{DIS}}(x, \mathbf{k}^2, \mathbf{q}^2) \Phi_p \left( \frac{\mathbf{q}^2}{Q_0^2} \right). \quad (2.2)$$

In Mellin space conjugate to transverse momentum this gluon density can be written as

$$G(x, \mathbf{k}^2, M) = \frac{1}{\mathbf{k}^2} \int_{\frac{1}{2}-i\infty}^{\frac{1}{2}+i\infty} \frac{d\gamma}{2\pi i} \hat{g} \left( x, \frac{M^2}{Q_0^2}, \frac{\overline{M}^2}{M^2}, \gamma \right) \left( \frac{\mathbf{k}^2}{Q_0^2} \right)^\gamma. \quad (2.3)$$

$M$  is a characteristic hard scale of the process and  $\overline{M}$  a corresponding scale which enters the running coupling constant; in the DIS analysis  $M = \overline{M}$  and both scales have been identified with the virtuality of the scattering photon.  $\hat{g}$  is finally an operator in  $\gamma$  space and defined as

$$\hat{g} \left( x, \frac{M^2}{Q_0^2}, \frac{\overline{M}^2}{M^2}, \gamma \right) = \frac{\mathcal{C} \cdot \Gamma(\delta - \gamma)}{\pi \Gamma(\delta)} \cdot \left( \frac{1}{x} \right)^{\chi(\gamma, \frac{\overline{M}^2}{M^2})} \cdot \left\{ 1 + \frac{\bar{\alpha}_s^2 \beta_0 \chi_0(\gamma)}{8N_c} \log \left( \frac{1}{x} \right) \left[ -\psi(\delta - \gamma) + \log \frac{M^2}{Q_0^2} - \partial_\gamma \right] \right\}, \quad (2.4)$$

where  $\bar{\alpha}_s = \alpha_s N_c / \pi$  with  $N_c = 3$  the number of colors and  $\chi(\gamma, \overline{M}^2/M^2)$  is the next-to-leading logarithmic (NLL) BFKL kernel after collinear improvements; in addition large terms proportional to the first coefficient of the QCD beta function,  $\beta_0 = 11N_c/3 - 2n_f/3$  have been resummed through employing a Brodsky-Lepage-Mackenzie (BLM) optimal scale setting scheme [6]. The NLL kernel with collinear improvements reads

$$\chi \left( \gamma, \frac{\overline{M}^2}{M^2} \right) = \bar{\alpha}_s \chi_0(\gamma) + \bar{\alpha}_s^2 \left[ \tilde{\chi}_1(\gamma) - \frac{\chi_0'(\gamma) \chi_0(\gamma)}{2} - \frac{\beta_0 \chi_0(\gamma)}{8N_c} \log \frac{\overline{M}^2}{M^2} \right] + \chi_{RG}(\bar{\alpha}_s, \gamma, \tilde{a}, \tilde{b}). \quad (2.5)$$

with the leading-order BFKL eigenvalue,  $\chi_0(\gamma) = 2\psi(1) - \psi(\gamma) - \psi(1 - \gamma)$ . The term proportional to  $\log \overline{M}^2/M^2$  in Eq. (2.5) has been introduced as a new element w.r.t. [4] and [5], and takes into account that the scale of the running coupling ( $\overline{M}$ ) and the hard scale ( $M$ ) are not necessarily identical.  $\chi_{RG}$  achieves a resummation of terms enhanced by (anti-)collinear logarithms in the NLO kernel and reads [4, 7].

$$\chi_{RG}(\bar{\alpha}_s, \gamma, a, b) = \bar{\alpha}_s (1 + a\bar{\alpha}_s) (\psi(\gamma) - \psi(\gamma - b\bar{\alpha}_s)) - \frac{\bar{\alpha}_s^2}{2} \psi''(1 - \gamma) - \frac{b\bar{\alpha}_s^2 \cdot \pi^2}{\sin^2(\pi\gamma)} + \frac{1}{2} \sum_{m=0}^{\infty} \left( \gamma - 1 - m + b\bar{\alpha}_s - \frac{2\bar{\alpha}_s(1 + a\bar{\alpha}_s)}{1 - \gamma + m} + \sqrt{(\gamma - 1 - m + b\bar{\alpha}_s)^2 + 4\bar{\alpha}_s(1 + a\bar{\alpha}_s)} \right). \quad (2.6)$$

$\tilde{\chi}_1$  denotes the 1-loop corrections to the BFKL eigenvalue. Adopting BLM optimal scale setting and the momentum space (MOM) physical renormalization scheme with  $Y \simeq 2.343907$  and gauge

parameter  $\xi = 3$  it reads, see also the discussion in [8]

$$\tilde{\chi}_1(\gamma) = \tilde{\mathcal{S}}\chi_0(\gamma) + \frac{3}{2}\zeta(3) + \frac{\Psi''(\gamma) + \Psi''(1-\gamma) - \phi(\gamma) - \phi(1-\gamma)}{4} - \frac{\pi^2 \cos(\pi\gamma)}{4 \sin^2(\pi\gamma)(1-2\gamma)} \cdot \left[ 3 + \left(1 + \frac{n_f}{N_c^3}\right) \frac{2+3\gamma(1-\gamma)}{(3-2\gamma)(1+2\gamma)} \right] + \frac{1}{8} \left[ \frac{3}{2}(Y-1)\xi + \left(1 - \frac{Y}{3}\right)\xi^2 + \frac{17Y}{2} - \frac{\xi^3}{6} \right] \chi_0(\gamma), \quad (2.7)$$

where  $\tilde{\mathcal{S}} = \frac{(4-\pi^2)}{12}$  and

$$\phi(\gamma) + \phi(1-\gamma) = \sum_{m=0}^{\infty} \left( \frac{1}{\gamma+m} + \frac{1}{1-\gamma+m} \right) \left[ \Psi' \left(1 + \frac{m}{2}\right) - \Psi' \left(\frac{1+m}{2}\right) \right]. \quad (2.8)$$

The coefficients  $\tilde{a}, \tilde{b}$  which enter  $\chi_{\text{RG}}$  Eq. (2.6) are obtained as the coefficients of the  $1/\gamma$  and  $1/\gamma^2$  poles of the NLO eigenvalue with

$$\begin{aligned} \tilde{a} &= -\frac{13}{36} \frac{n_f}{N_c^3} - \frac{55}{36} + \frac{3Y-3}{16} \xi + \frac{3-Y}{24} \xi^2 - \frac{1}{48} \xi^3 + \frac{17}{16} Y \\ \tilde{b} &= -\frac{n_f}{6N_c^3} - \frac{11}{12}. \end{aligned} \quad (2.9)$$

Due to the BLM optimal scale setting, the running coupling turns into an element dependent on the Mellin-variable  $\gamma$ :

$$\tilde{\alpha}_s(\bar{M} \cdot Q_0, \gamma) = \frac{4N_c}{\beta_0 \left[ \log \left( \frac{\bar{M} \cdot Q_0}{\Lambda^2} \right) + \frac{1}{2} \chi_0(\gamma) - \frac{5}{3} + 2 \left(1 + \frac{2}{3} Y\right) \right]}; \quad (2.10)$$

in addition – in order to access the region of relatively small hard scales – in [4], a parametrization of the running coupling has been used [9],

$$\alpha_s(\mu^2) = \frac{4\pi}{\beta_0 \ln \frac{\mu^2}{\Lambda^2}} + f \left( \frac{\mu^2}{\Lambda^2} \right), \quad f \left( \frac{\mu^2}{\Lambda^2} \right) = \frac{4\pi}{\beta_0} \frac{125 \left(1 + 4 \frac{\mu^2}{\Lambda^2}\right)}{\left(1 - \frac{\mu^2}{\Lambda^2}\right) \left(4 + \frac{\mu^2}{\Lambda^2}\right)^4}. \quad (2.11)$$

### 3. Comparison to data & conclusion

In Fig. 1 and Fig. 2 we compare perturbative BFKL evolution driven by the BFKL gluon with  $x = M_V^2/(W^2 - m_p^2)$  (where  $M_V$  is the mass of the vector meson and  $m_p$  the proton mass) to experimental data. Even though we require in the case of the  $J/\Psi$  a  $K$ -factor of the order of 0.8 to address an off-set in the overall normalization, we find that the  $W$ -dependence of the total exclusive vector meson photo-production cross-section is both for  $J/\Psi$  and  $\Upsilon$  production very well described in terms of collinear improved BFKL evolution. As a new feature we included in the present comparison 2016 13 TeV LHCb data. In accordance with the 2014 LHCb data se, they seem to prefer the choice  $M^2 = (M_{J/\Psi}/2)^2$  for the hard scale. The good agreement with the data seems to suggest that at currently accessible collider data non-linear effects are not yet dominant. Nevertheless care is needed in the interpretation of these results: at first the uncertainty band of the BFKL prediction increases in the region of largest  $W$  value (in particular in the case of the  $J/\Psi$

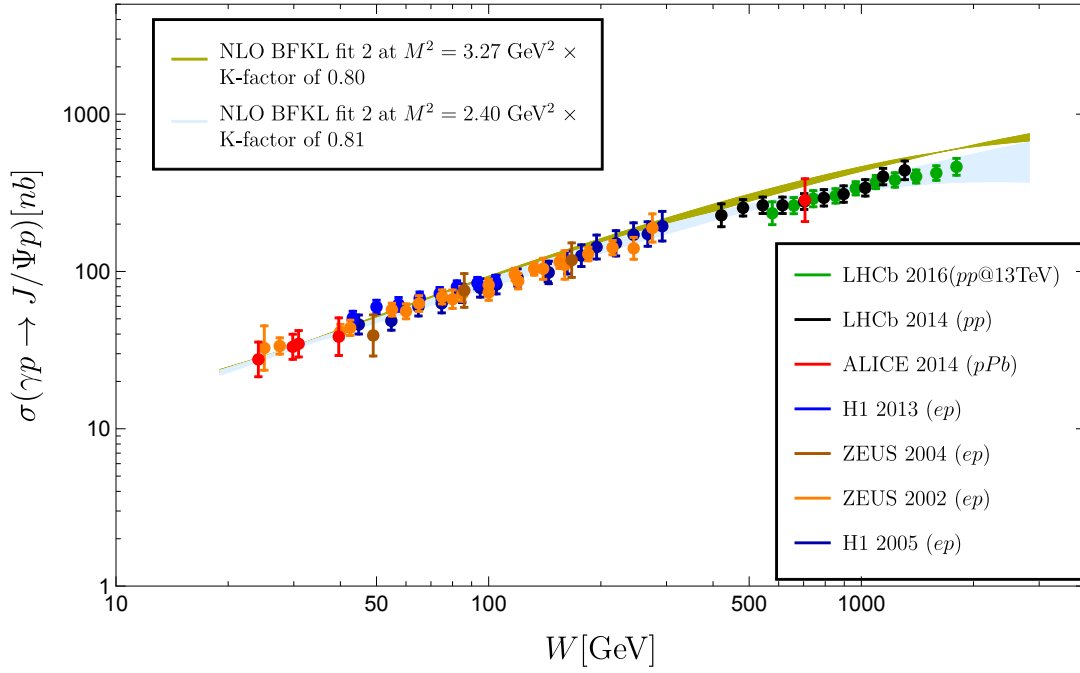


**Figure 1:** Energy dependence of the  $J/\Psi$  photo-production cross-section as provided by the BFKL fit 1 (up) and 2 (down). The uncertainty band reflects a variation of the scale  $\bar{M}^2 \rightarrow \{\bar{M}^2/2, \bar{M}^2 \cdot 2\}$ . We also show photo-production data measured at HERA by ZEUS [10] and H1 [11] as well as LHC data obtained from ALICE [12] and LHCb ( $W^+$  solutions) [13].

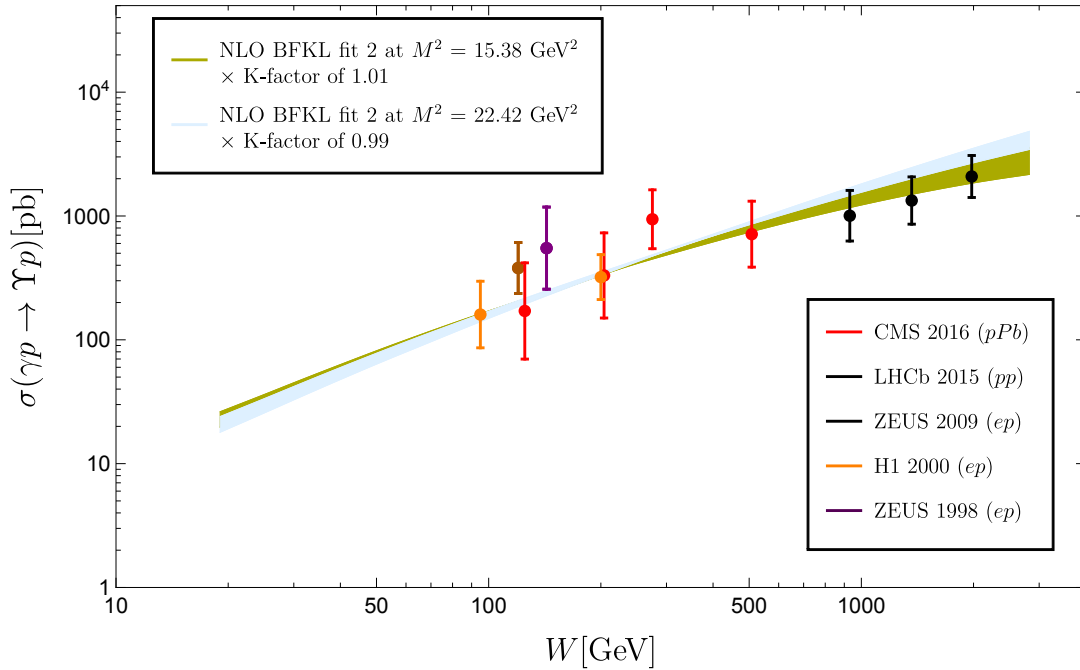


**Figure 2:** Energy dependence of the  $\Upsilon$  photo-production cross-section as provided by the BFKL fit 1 (up) and 2 (down). The uncertainty band reflects a variation of the scale  $\bar{M}^2 \rightarrow \{\bar{M}^2/2, \bar{M}^2 \cdot 2\}$ . We also show HERA data measured by H1 [14] and ZEUS [15] and LHC data by LHCb [16] and CMS [17].

which is characterized by a smaller hard scale). This indicates the existence of a potential instability of the current implementation of NLO BFKL evolution in this region of phase space. Moreover, non-linear effects are for exclusive vector meson production only manifest through evolution, but not on the level of the observable. This suggests that it is necessary to identify observables which are sensitive to saturation effects already at the level of the observables to allow for improved saturation searches, see *e.g.* [18] for a recent calculation and a related discussion.

## References

- [1] I. Bautista, A. Fernandez Tellez and M. Hentschinski, *Phys. Rev. D* **94** (2016) no.5, 054002 [arXiv:1607.05203 [hep-ph]].
- [2] S. P. Jones, A. D. Martin, M. G. Ryskin and T. Teubner, *J. Phys. G* **41**, 055009 (2014) [arXiv:1312.6795 [hep-ph]]; *JHEP* **1311**, 085 (2013) [arXiv:1307.7099].
- [3] N. Armesto and A. H. Rezaeian, *Phys. Rev. D* **90**, no. 5, 054003 (2014) [arXiv:1402.4831]; V. P. Goncalves, B. D. Moreira and F. S. Navarra, *Phys. Rev. C* **90**, no. 1, 015203 (2014) [arXiv:1405.6977].
- [4] M. Hentschinski, A. Sabio Vera and C. Salas, *Phys. Rev. Lett.* **110** (2013) no.4, 041601 [arXiv:1209.1353 [hep-ph]]; *Phys. Rev. D* **87** (2013) no.7, 076005 [arXiv:1301.5283 [hep-ph]].
- [5] G. Chachamis, M. Deàk, M. Hentschinski, G. Rodrigo and A. Sabio Vera, *JHEP* **1509**, 123 (2015) [arXiv:1507.05778 [hep-ph]].
- [6] S. J. Brodsky, G. P. Lepage and P. B. Mackenzie, *Phys. Rev. D* **28** (1983) 228.
- [7] G. P. Salam, *JHEP* **9807** (1998) 019 [hep-ph/9806482]; A. Sabio Vera, *Nucl. Phys. B* **722** (2005) 65 [hep-ph/0505128].
- [8] S. J. Brodsky, V. S. Fadin, V. T. Kim, L. N. Lipatov and G. B. Pivovarov, *JETP Lett.* **70** (1999) 155 [hep-ph/9901229].
- [9] B. R. Webber, *JHEP* **9810** (1998) 012 [hep-ph/9805484].
- [10] S. Chekanov *et al.* [ZEUS Collaboration], *Eur. Phys. J. C* **24**, 345 (2002) [hep-ex/0201043]; *Nucl. Phys. B* **695**, 3 (2004) [hep-ex/0404008].
- [11] C. Alexa *et al.* [H1 Collaboration], *Eur. Phys. J. C* **73**, no. 6, 2466 (2013) [arXiv:1304.5162 [hep-ex]]; *Eur. Phys. J. C* **46**, 585 (2006) [hep-ex/0510016].
- [12] B. B. Abelev *et al.* [ALICE Collaboration], *Phys. Rev. Lett.* **113**, no. 23, 232504 (2014) [arXiv:1406.7819 [nucl-ex]].
- [13] R. Aaij *et al.* [LHCb Collaboration], *J. Phys. G* **40**, 045001 (2013) [arXiv:1301.7084 [hep-ex]]; *J. Phys. G* **41**, 055002 (2014) [arXiv:1401.3288 [hep-ex]].
- [14] C. Adloff *et al.* [H1 Collaboration], *Phys. Lett. B* **483**, 23 (2000) [hep-ex/0003020].
- [15] J. Breitweg *et al.* [ZEUS Collaboration], *Phys. Lett. B* **437** (1998) 432 [hep-ex/9807020]; *Phys. Lett. B* **680**, 4 (2009) [arXiv:0903.4205 [hep-ex]].
- [16] R. Aaij *et al.* [LHCb Collaboration], *JHEP* **1509**, 084 (2015) [arXiv:1505.08139 [hep-ex]].
- [17] CMS Collaboration [CMS Collaboration], “Measurement of exclusive Y photoproduction in pPb collisions at  $\sqrt{s_{NN}} = 5.02$  TeV,” CMS-PAS-FSQ-13-009.
- [18] A. Ayala, M. Hentschinski, J. Jalilian-Marian and M. E. Tejeda-Yeomans, *Phys. Lett. B* **761** (2016) 229 [arXiv:1604.08526 [hep-ph]]; *Nucl. Phys. B* **920** (2017) 232 [arXiv:1701.07143 [hep-ph]].